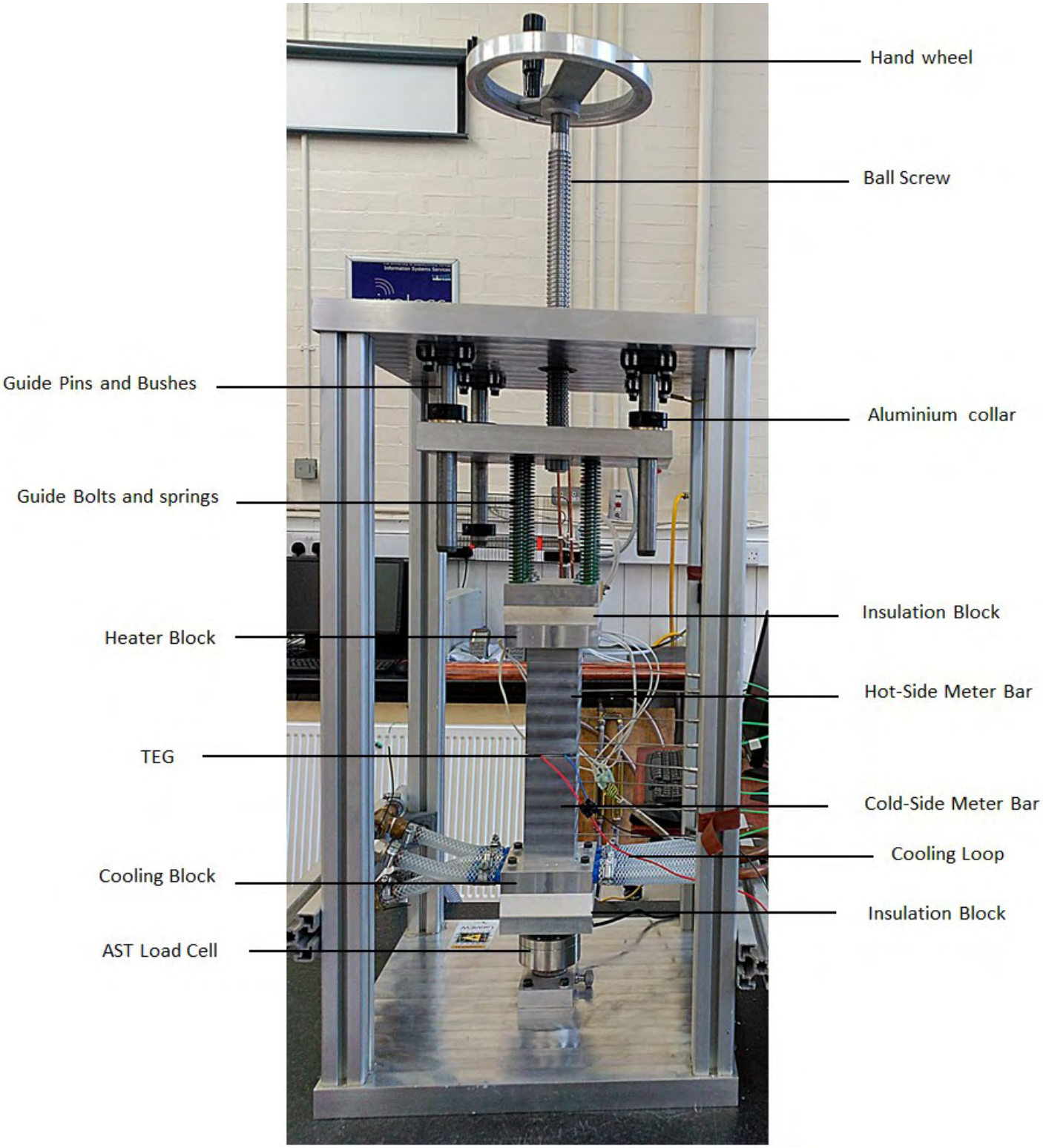

Figure 11: Assembled test rig

The hand wheel is used to provide a smooth and gradual application of load. Four adjustable aluminium collars above the driver plate allow to maintain the compressive load. After turning the hand wheel to apply the required force the four aluminium collars are tightened onto the guide pins to prevent the driver plate from moving back up (due to the springs force witch force the driver plate upwards).

Cooling Loop

The cooling block is plumb into a cooler (Figure 12). Pipe connecters connect inlets and outlets of the cooling block to the cooler. The cooler is a Grant RC 1400G with a cooling power 1.1 kW at 20°C ambient air temperature. It is capable of providing water to the cooling block at 10°C at a rate of 15 L/min.

Figure 12: Grant RC 1400G Cooler

Heater Block

Four cartridge heaters are inserted into the heater block. The cartridge heaters are connected in parallel to a potentiometer (Carrol and Meynell CMV10E-1 variac). Two multimeters (ISOTECH M91E Voltage Reading Multimeter) allow the reading of the voltage and current output from the variac (Figure 13).

Figure 13: Power Supply to Cartridge Heaters

Load resistance

An electric load (Figure 14) is connected to the TEGs outputs to allow its electrical characterisation in closed-circuit. The load is the model 8540 DC of BK Precision. It can operate in CC, CV or CR mode while voltage/current or resistance/power values are measured and displayed in real time.

Figure 14: Electronic Load

Instrumentation

Temperature measurements along the aluminium meter bars are made by 8 K-type thermocouples (Figure 15).

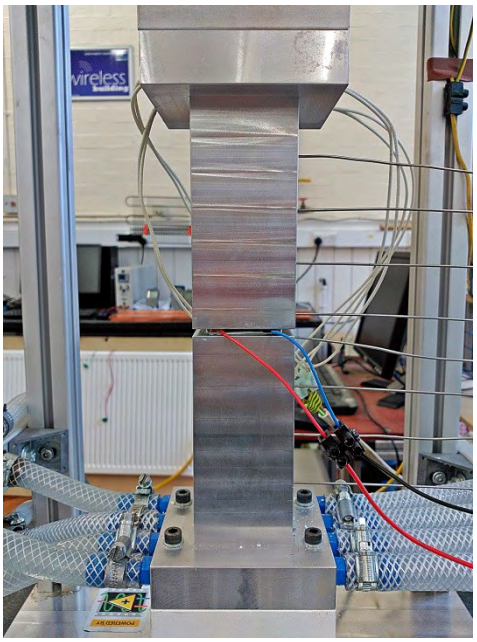

Figure 15: Aluminium meter bars

An AST KAF-W load cell measures the clamping force on the TEG. It requires an excitation voltage of 20V which is supplied by an EX2020R power supply unit.

Finally, an NI9219 DAQ is used to measure the output signal from the load cell and the TEG under test. The DAQ has four channels with channel-to channel isolation. This channel isolation prevents a stacking of the common mode voltage and reduces signal noise. The DAQs are connected to a PC with LabVIEW software to record all relevant data.

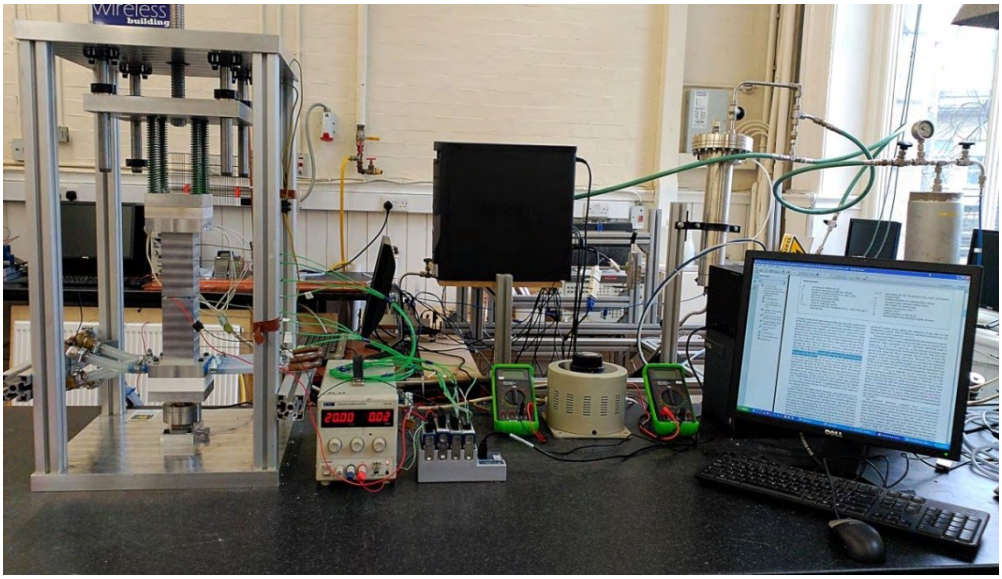

Figure 16: Experimental Rig and Instrumentation

Temperature controller

The temperature difference across the TEG must be maintained constant to obtain an electrical characterisation of the thermoelectric device.

The idea was to use a temperature controller (Figure 17). This advice allows to maintain a constant temperature of a thermocouple by adjusting the power of the potentiometer. To control the temperature difference between thermocouples T5 and T4 (Figure 15) a connexion in series with both thermocouples was made as shown in Figure 18.

Figure 17: PID temperature controller (CAL 9900)

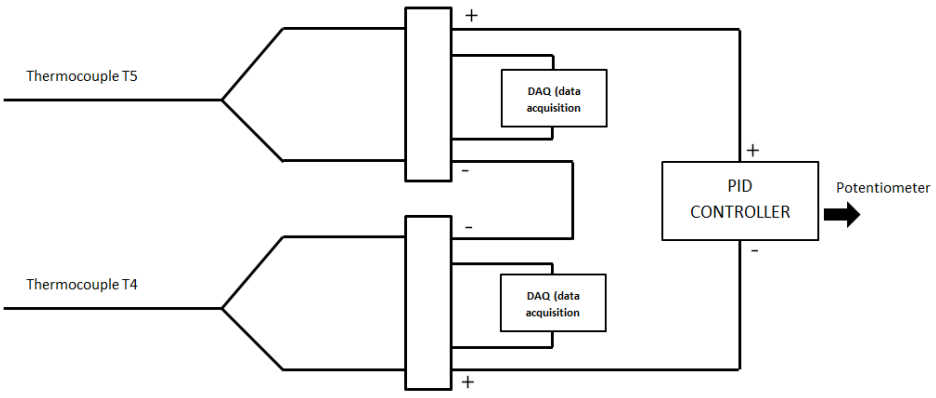

Figure 18: Series connexion of two thermocouples

Uncertainty of measurement

Table 1 shows a summary of the measuring instruments used in the rig with their units and measurement uncertainties:

Source of uncertainty	Parameter	Notation	Units	Measurement uncertainty (±% of value)
AST KAF-W Load Cell	Pressure	P	kN	±0.05%
8540 DC Load Resistance	Resistance	R	Ω	±(1%+0.8%FS)
	Voltage	V	V	±(0.05%+0.1%FS)
	Current	I	A	±(0.11%+0.1 %FS)
ISOTECH M91E Voltage Reading Multimeter	Voltage	V	V	±1.25%+4Digits
	Current	I	A	±1.5%+3Digits
Grant RC 1400G Chiller	Temperature	T	ºC	±0.25%

Table 1: Accuracy of measuring instruments used

3.2. Temperature testing: energy balance across the TEG

This part of the project focuses on the energy balance across the TEG in order to understand how the power generated can be obtained using heat transfer equation once the steady-state is achieved.

The use of meter bars allows the TEG surface temperature to be determined through extrapolation. The hot and the cold side temperature for the TEG surface can be read from Figure 19 by extrapolating the temperature to zero distance (x-axis intercept).

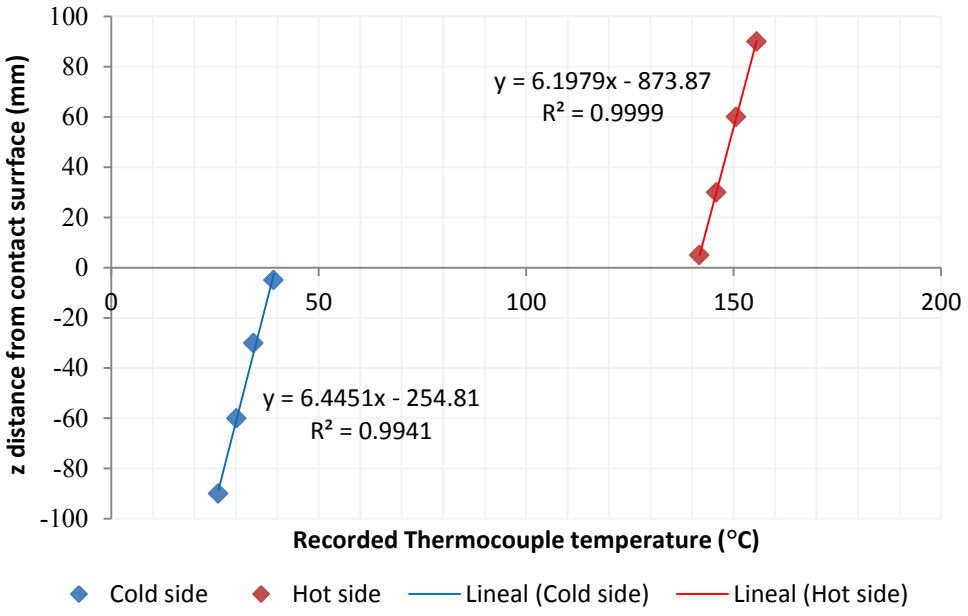

Figure 19: Temperatures along Meter bar length when 150 W of power are applied in open circuit. The temperature of the chiller is fixed to 21°C and the applied pressure 0.378 Mpa.

The inverse of the gradient of the line for each meter bar represents the change of temperature with position z. After a certain amount of equilibrium time when the heat flow through the meter bars reaches a steady state this value become constant. It is then possible to calculate the heat flux $\vec{q}$ (W/m^2) through each bar using Fourier's law conduction:

$$\vec{q} = k\left(\frac{dT}{dz}\right) \tag{14}$$

Where k is the thermal conductivity of the material (W/mK), T is temperature (K) and z is position along the meter bars (m).

As the cross sectional area A of the meter bars is known, assuming one dimensional heat flow, it is possible to calculate the heat flux per unit time Q as:

$$\dot{Q} = -kA\left(\frac{\Delta T}{\Delta z}\right) \tag{15}$$

With heat flow rate through the hot and cold meter bars quantified, $\dot{Q}_H$ and $\dot{Q}_C$, it's then possible to compare these results with the power output of the TEG P_{elec} , and conduct energy balance across the module.

$$P_{elec} = \dot{Q}_H - \dot{Q}_C \tag{16}$$

However, the equation 16 was not used in this project due to the difficulty in quantifying the heat flow (the thermal conductivity of the meter bars is uncertain, in addition, meter bars dissipate power by radiation and convection). Instead, the electrical power was quantified by measuring the voltage and current of the external load resistance.

3.3. Pressure testing

The objective is to evaluate the influence of the pressure on TEG performance. The compressive load is increased from 0.25 MPa to 0.75 MPa (which corresponds to 40 and 120 kgf on a surface of 40x40 mm^2) and decreased again. The open-circuit voltage is measured in each load point.

Figure 20 shows that the output TEG voltage increases with the pressure. In fact, the mechanical pressure reduces the thermal contact resistance between the TEG and the meter bars and it directly influences the amount of power produced (18).

Henceforth, every test is performed imposing 1MPa of mechanical pressure onto the TEG to minimize the contact resistance. A more important value might be destructive for the delicate thick ceramic plate because of the thermal expansion (20).

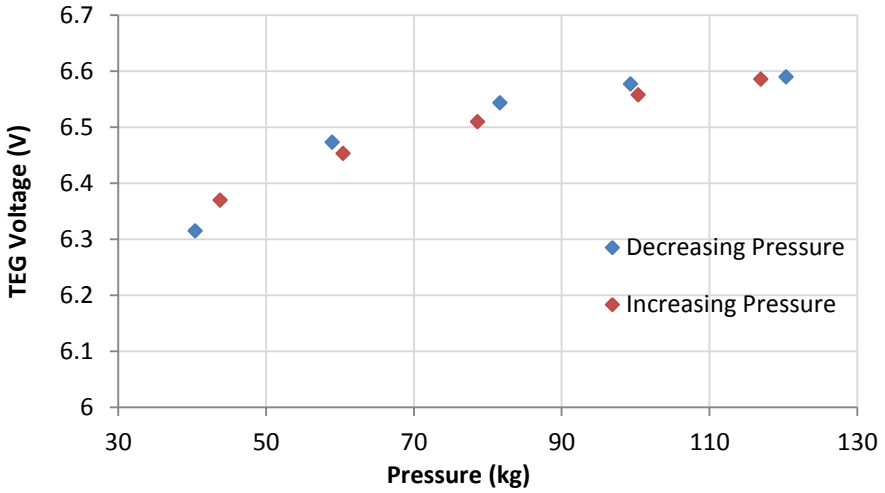

Figure 20: Voltage as a function of pressure for 130°C of temperature difference across the TEG in open circuit. The temperature of the cooler was fixed at 19 °C.

3.4. Electrical characterisation of the TEG

Electrical characterisation of the TEG refers to measurement of its voltage-vs-current and power-vs-current curves, to describe its ready-state performance and electrical behaviour under different loading resistance conditions.

The first part of this section analyse the case in which the temperature difference across the module is constant. This type of characterisation is an established method to specify the performance of TEG devices. However, when physically obtaining this characterisation it is necessary to analyse the difference case in which the heat input is constant and the temperature different across the TEG varies depending on its effective thermal resistance. This

situation occurs in most waste heat recovery applications because the available thermal power is at any time limited.

3.4.1. Measurement protocol

When the temperature difference across the module is constant the experimental methodology is as shown in the scheme 1:

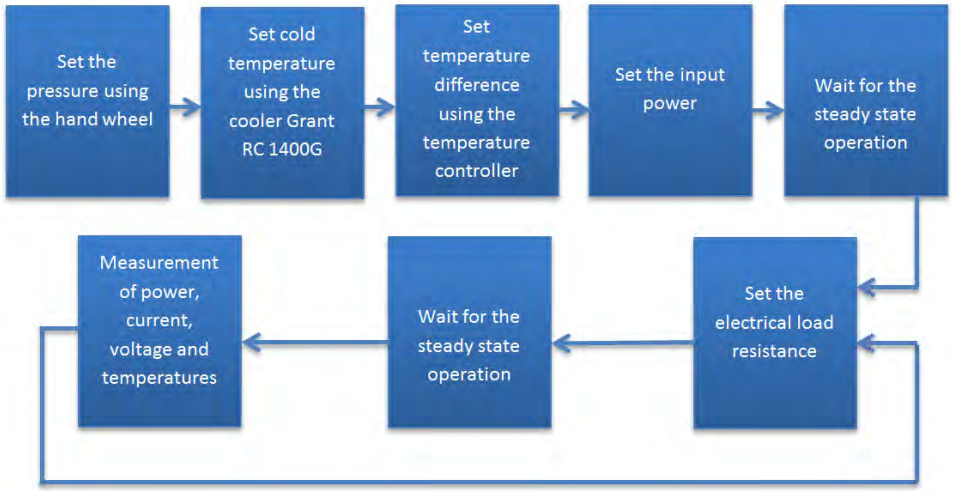

Scheme 1: Protocol of the electrical characterisation when temperature difference is constant

When the heat input is constant the experimental methodology is as shown in the scheme 2.

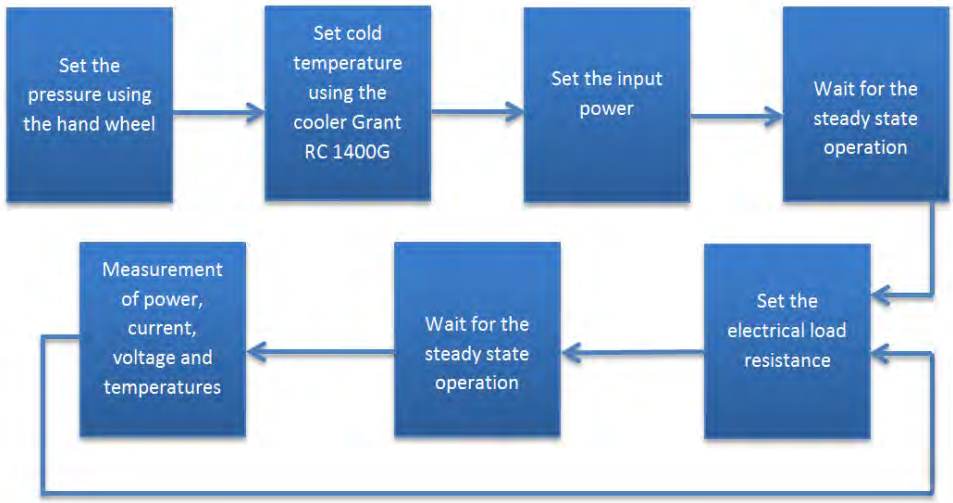

Scheme 2: Protocol of the electrical characterisation when heat input is constant

3.4.1- Theoretical models for constant temperature across the TEG

This section describes the steady-state behaviour of the TEG when constant temperatures are maintained at its faces.

The operation of thermoelectric devices depends on three main effects:

- Thermal conduction
- Seebeck effect
- Internal Joule heating

The Seebeck coefficient is assumed to have the same (constant) magnitude in both types of pellets, but its sign is positive in p-type pellets and negative in n-type pellets. Since the Seebeck coefficients are constant the Thomson effect is not present (21).

Using the standard model and assuming one dimensional conduction through the module, the rate of heat supply $\dot{Q_H}$ can be estimated at the hot junctions as:

$$\dot{Q_H} = \frac{kA(\Delta T)}{L} + (\alpha_{p,n})T_H I - \frac{1}{2}R_{int}I^2 \quad (17)$$

Where

k: Overall conduction coefficient
A: Cross sectional area of the module
ΔT: Temperature gradient across the module
L: Thickness of the TEG
$\alpha_{p,n}$: Seebeck coefficient ($\alpha_{p,n} = \alpha_p - \alpha_n$)
T_H: Temperature at the hot side
I: Current produced
R_{int}: Overall resistance of the device

The equation 17 is derived from the steady-state solution of the one-dimensional heat conduction equation for solids with internal energy generations. The full demonstration is found in Appendix A.1.

The solution for the cold side is similar. This result shows that the Joule heating is equally divided between the hot and cold sides.

$$\dot{Q_C} = \frac{kA(\Delta T)}{L} + (\alpha_{p,n})T_C I - \frac{1}{2}R_{int}I^2 \quad (18)$$

By applying an energy balance across the module, the electrical power generated by the TEG, P_{elec}, is equal to the difference between heat delivered and dissipated

$$P_{elec} = \dot{Q_H} - \dot{Q_C} = (\alpha_{p,n})I\Delta T - I^2 R_{int} \quad (19)$$

Dividing across by the current gives the voltage:

$$\boldsymbol{V = \alpha_{p,n}\Delta T - IR_{int}} \quad (20)$$

This gives voltage as a function of current for a given temperature difference. Using the standard model, the parameter $\alpha_{p,n}$ is measured by open-circuiting (I=0) the TEG, and measuring the applied temperature difference and corresponding voltage. By setting P_{elec} equal to $I^2 R_L$ (where R_L is the load resistance) in equation 19, the current can be found from

$$I = \frac{\alpha_{p,n}\Delta T}{(R_L + R_{int})} \quad (21)$$

Substituting Equation 21 into Equation 19 yields an expression for the electrical power

$$\boldsymbol{P_{elec} = (\alpha_{p,n}\Delta T)^2 \frac{R_L}{(R_L + R_{int})^2}} \quad (22)$$

A thermoelectric module generates maximum power when the module resistance matches the load resistance, i.e. when $R_L = R_{int}$. The demonstration is shown in Appendix A.2. It follows that the maximum power,P_{max}, is given by

$$P_{max} = \frac{(\alpha_{p,n}\Delta T)^2}{4R_{int}} = \frac{A(\alpha_{p,n}\Delta T)^2}{8\rho L} \quad (23)$$

From Equation 23, the power produced by each thermocouple is approximately proportional to its cross-sectional area, and inversely proportional to its length.

Rowe and Min (22) developed a theoretical model which also took into account the electrical and thermal contact resistances across the ceramic and conductive strips, but this model requires detailed knowledge of the contact parameters and the physical properties of the p-n pellets – information that is not always available from the manufacturer or supplier.

For this study, an approach used by Hsu et al. (23) is utilized. This method known as the effective Seebeck coefficient model, calculates the Seebeck coefficient under actual load conditions. This is necessary since the TEG performs differently under open-circuit and load settings.

To calculate the effective Seebeck coefficient a fixed temperature is applied across the TEG and the load resistance is varied. For the TEG used in this study (TG12-8 from *Marlow industries)*, Figure 21 plots the voltage vs. the current for a range of temperature differences.

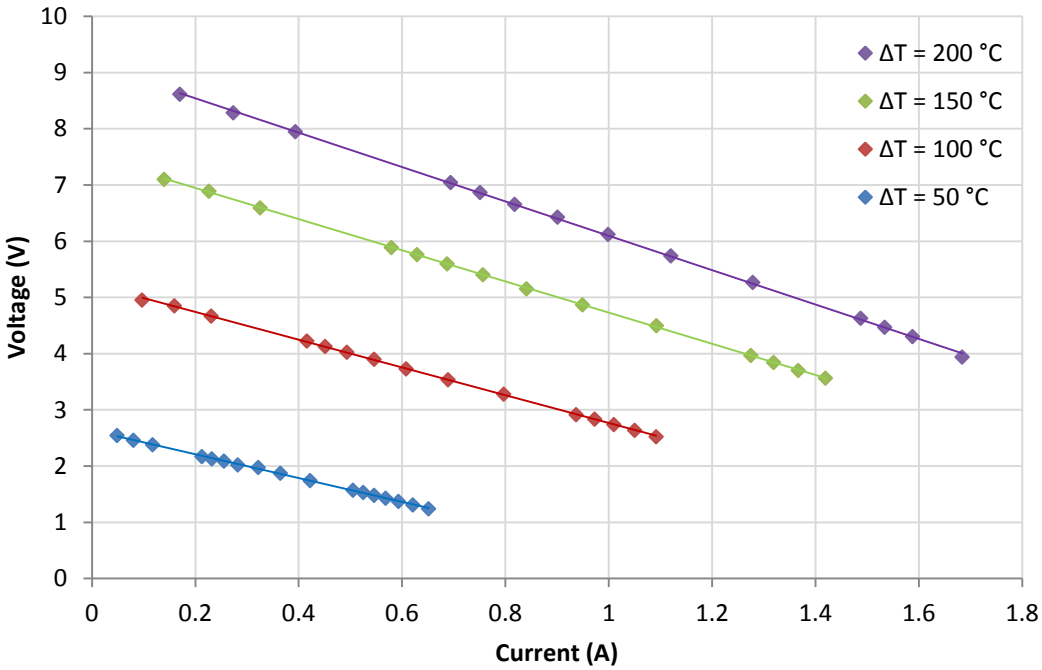

Figure 21: Voltage vs. current for a range of temperature differences

A linear relationship exists between the voltage and current. The "effective" open-circuit voltage can be read from Figure 21 by extrapolating the voltage corresponding to zero current (y-axis intercept). Similar to Equation 20 the approach of Hsu et al. relates the voltage and the current:

$$V = \alpha_{p,n}\Delta T - R_{int}I = A\Delta T - BI \tag{24}$$

It is important to highlight that this electrical characteristic is linear because the values of both the Seebeck coefficient and the internal resistance are constant (they use to vary with temperature however the temperature across the TEG device is constant in this section).

This equation is equivalent to the electrical configuration in Figure 22.

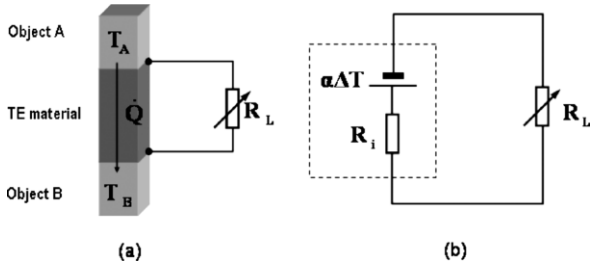

Figure 22: Principle of variable thermal resistor. (a) Thermoelectric material sandwiched between two thermal bodies and connected to a variable electrical resistor and (b) equivalent thermoelectric circuit for the structure shown in (a) (24).

For the open-circuit voltage ($I = 0$), $A\Delta T$ has a maximum value in which A can be defined as the effective Seebeck coefficient α_{eff}.

$$\alpha_{eff} = \frac{V_{oc}}{\Delta T} \tag{25}$$

The effective Seebeck coefficient specifies the TEG behaviour under actual load conditions, indirectly taking into account the contact effects such as interfacial temperature drops which are not measured in this study.

The power may be calculated from the following equation:

$$\boldsymbol{P_{elec} = (\alpha_{eff}\Delta T)^2 \frac{R_L}{(R_L + R_{int})^2}} \tag{26}$$

Figure 23 plots the experimental data along with the theoretical predictions provided by the standard model (Equation 22) and the effective Seebeck coefficient model (Equation 26). Clearly, the effective Seebeck coefficient model predicts the TEG behaviour more accurately for the TEG used in this study.

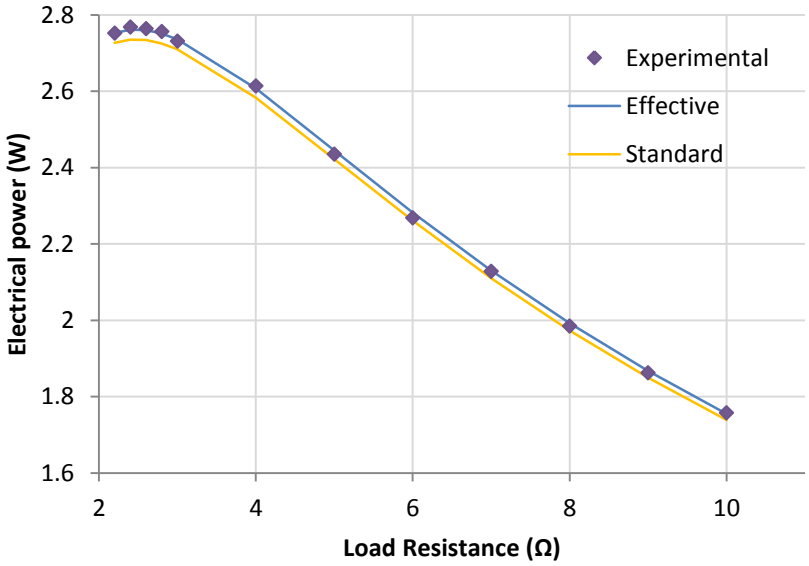

Figure 23- Measured and predicted TEG performance using the standard model and the effective Seebeck coefficient model when ΔT=100°C

Figure 24 shows the performance curve when the TEG operated at a temperature difference ΔT of 100 °C. The blue straight line represents the voltage versus current (V-I) characteristic, while the violet curved line is the power curve (P-I) for the device. The open circuit voltage V_{OC} is the voltage when no current is drawn by the load. The maximum point lies at the point when $V_{load} = \frac{V_{OC}}{2}$ and is established when the equivalent electrical load

resistance equals the internal electrical resistance of the TEG R_{int} (stated by the theorem maximum power transfer (25)).

When the TEG is operated to the left of the maximum power point as shown in Figure 24 reduced current flows through the TEG and the effective thermal conductivity of the TEG (which depends also on the current flow, due to the parasitic Peltier effect) decreases. Under this condition the thermal energy conducted via the TEG is less than at the maximum power point. This is advantageous in most circumstances since it leads to increased thermal efficiency of the system.

The thermal efficiency of the system is defined as:

$$\eta = \frac{Electrical\ power\ to\ the\ load}{Heat\ power\ absorbed\ at\ the\ hot\ jonction} = \frac{P_{out}}{\dot{Q}_H} \qquad (27)$$

When the TEG is operated to the right of the maximum power point the thermal conductivity increases and the thermal energy conducted via the TEG is greater than that which flows at the maximum power point. Operation in the region to the right leads to a reduced thermal efficiency of the system.

As shown in Figure 24 the maximum power is approximately 2.76 W with a corresponing output voltage of 2.67 V (being half of the open-circuit voltage of 5.20V).

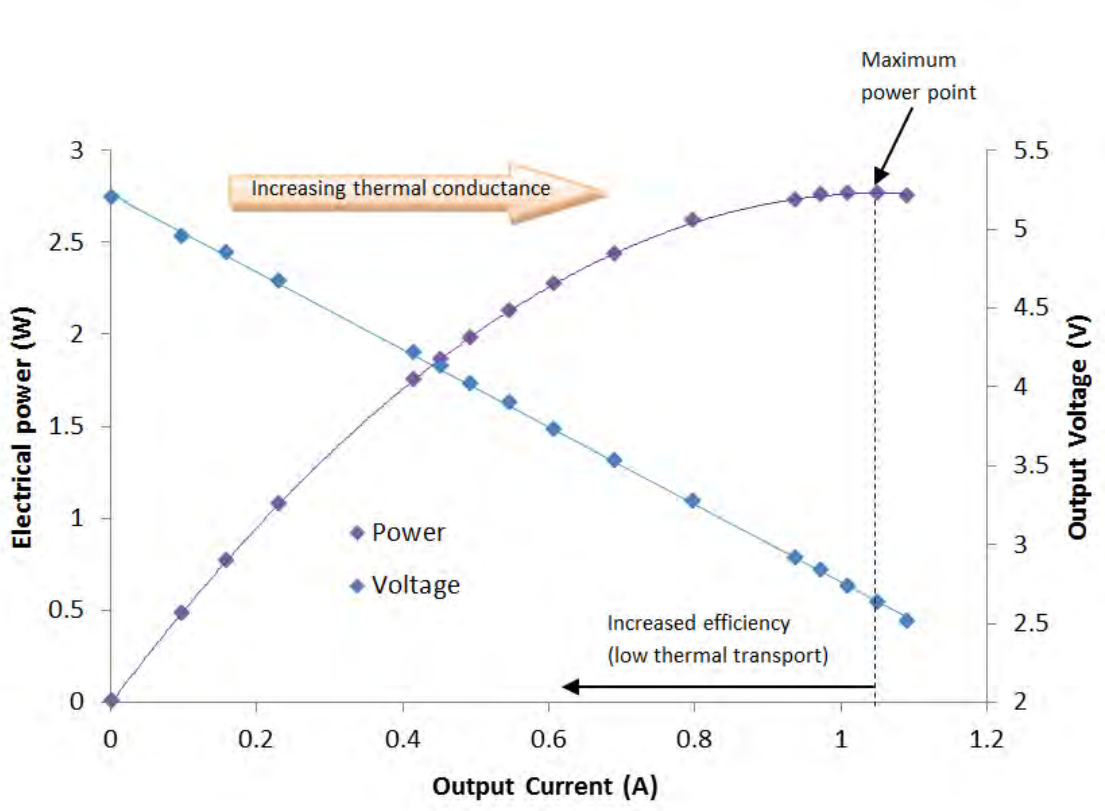

Figure 24: Electrical characterisation (VI and PI curves) of the TEG for ΔT=100°C

More data about electrical characterisation for different temperatures across the TEG are found in Appendix A.3.

3.4.2- Theoretical models for constant heat

This part of the project analyses the different case in which the input thermal is constant and the temperature difference across the TEG varies.

In Figure 25 it can be noted that the temperature difference decreases significantly with reducing load resistance (increasing current loads) due to an increase in heat pumped from the hot to the cold side. In fact, this additional heat flow is caused by the Peltier effect when there is an electric current flowing through the thermoelectric material (24).

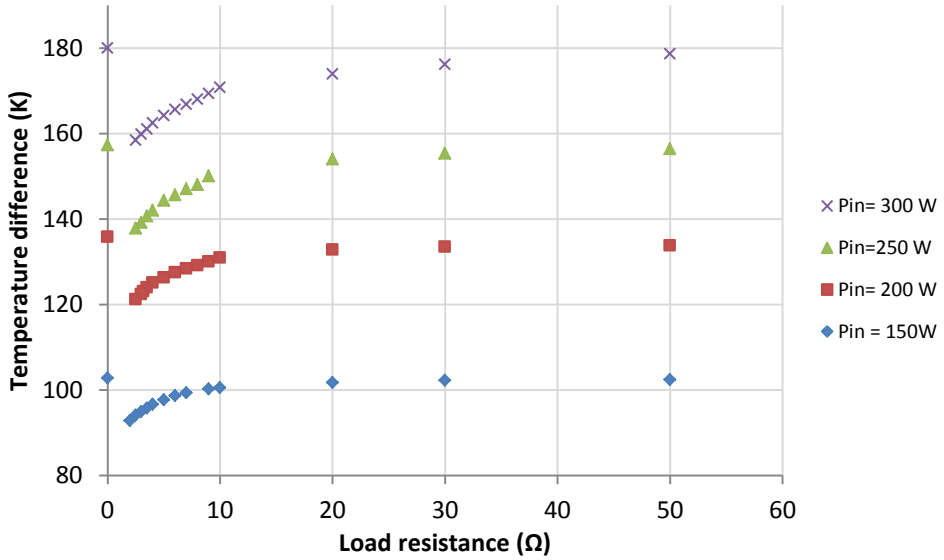

Figure 25: Temperature difference across the TEG as a function of load resistance

For a given temperature difference the electrical power delivered by the TEG varies depending on the current drawn by the electrical load connected to its terminals (Figure 24). It is known that to maximise the electrical power extracted from the TEG at any fixed temperature difference the load's impedance should equal the TEG's internal resistance. Hence the maximum power point lies at half of the open-circuit voltage V_{OC}.

The aim of this section is to proof if the voltage $V_{OC}/2$ which maximises power in constant temperature systems differs from the voltage that maximises power in constant heat operation.

The equation (20) assumed constant temperatures at the hot and cold side as boundary conditions. However, in constant heat characterisation both R_{int} and $\alpha_{p,n}$ vary with ΔT as shown in Figure 26.

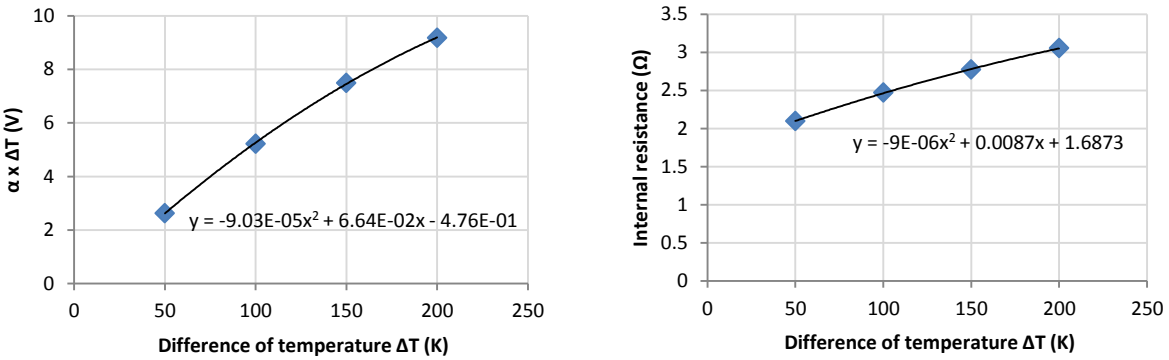

(a) *(b)*

Figure 26: Variation of internal resistance (a) and Seebeck Coefficient (b) with ΔT

It is possible to express their variation with ΔT using a 2nd-order polynomial equation, so that the load volage can be written as function of I_{load} and ΔT (26).

$$\boldsymbol{V_{load} = \left(a\Delta T^{\,2} + b\Delta T + c\right) - \left(d\Delta T^{\,2} + e\Delta T + f\right)I_{load}} \tag{28}$$

Where a, b, c, d, e and f are constant coefficients, different for each TEG and obtained from experimental data when the temperature difference is constant (Figure 26). They are listed in Table 2 for the TEG TG12-8 from *Marlow industries.*

Voc (V)			Rint (Ω)		
a (V/K^2)	b (V/K)	c (V)	d (Ω/K^2)	e (Ω /K)	f (Ω)
-9.03E-05	6.64E-02	-4.76E-01	-9.33E-06	8.68E-03	1.69E+00

Table 2

Using

$$\alpha_{p,n} = a\Delta T + b + \frac{c}{\Delta T} \tag{29}$$

$$R_{int} = d\Delta T^{\,2} + e\Delta T + f \tag{30}$$

In equation (17) results:

$$\dot{Q_H} = K(T_H - T_C) + \frac{a(T_H - T_C)^{\,2} + b(T_H - T_C) + c}{T_H - T_C} T_H I - \frac{d(T_H - T_C)^{\,2} + e(T_H - T_C) + f}{2} I^2 \tag{31}$$

Where K, which is the thermal conductance of the TEG in (W/K) at open-circuit, is considered constant because it is difficult to obtain confident measurements of it at different temperatures. Its variation might slightly affect the results presented here. It can be calculated as

$$K = \frac{\dot{Q_H}}{T_H - T_C} \tag{32}$$

Where $\dot{Q}_H$ is the thermal power flowing through the TEG, considered constant throughout this discussion.

In this study T_C can be considered constant without significant loss of accuracy (in fact its value is fixed by the cooler and varies slightly as a function of load resistance). This assumption is also realistic: in most TEG systems the cold side temperature remains almost constant with relatively small changes in thermal power flowing into the cold side. Also, this analysis facilitates the calculation of the temperature difference in equation 31.

The steady-state temperature difference is calculated solving Equation 31 by using iterative calculations in Excel, and the output power is then obtained by multiplying Equation 28 by the current I. Figure 27 shows the electrical power as a function of current for different values of heat input. It can be noted that the theoretical model predicts the TEG behaviour accurately.

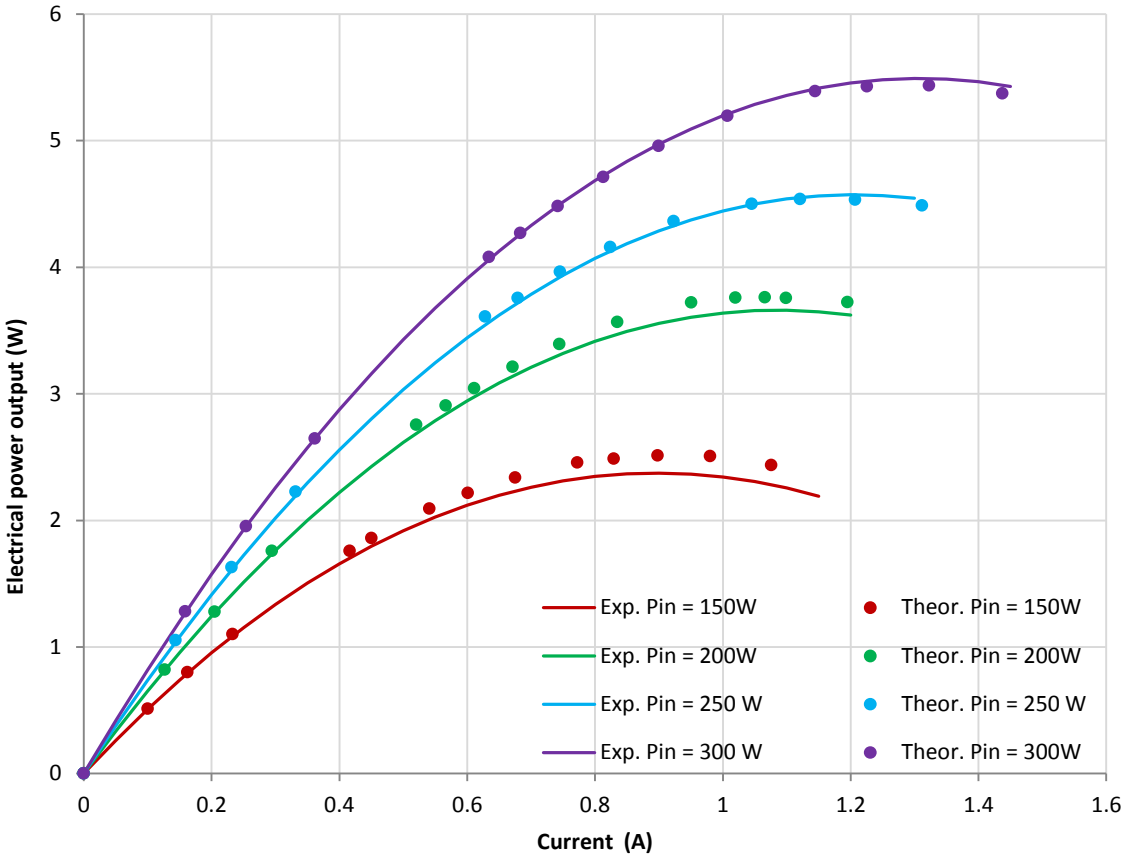

Figure 27: Electrical characterisation for a range of input power (Cold side temperature of 19°C)

Figure 28 shows the resulting electrical characterisation for 250 W of constant thermal power input; theoretical voltage as a fonction of current in green colour (on the secondary y-axis) and theoretical produced power in blue colour (on the primary y-axis).

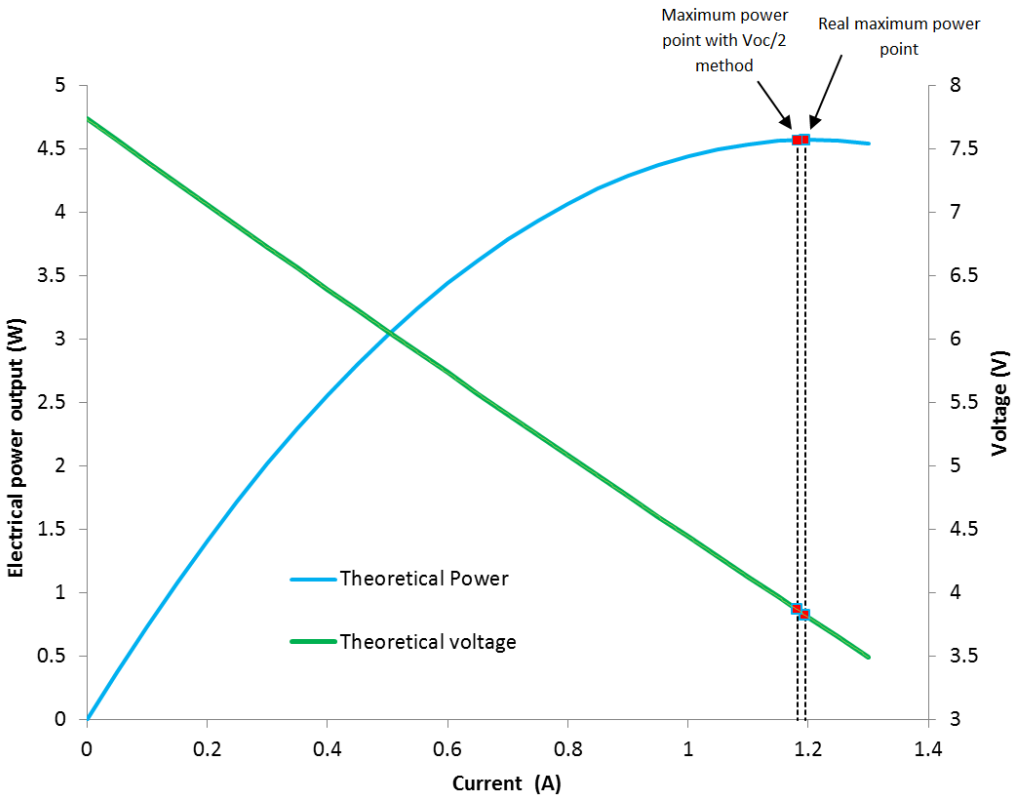

Figure 28: Electrical characterisation for a thermal input power of 250 W and temperature on the cold side of 19°C

It can be noted that the real maximum power is obtained for V_{MP}=3.838 V which is almost half of the initial open-circuit steady-state voltage V_{OCinit}/2= 3.869 V. Hence it is found that the real maximum power point is around 0.5 times the steady-state open-circuit voltage, V_{OCinit} , and that this relationship holds similarly when heat input is different.

Chapter 4: Design of the generator prototype

This part of the project consists of the design, construction, testing and evaluation of the thermoelectric device.

Due to the low heat emissions of the cook stove, the electricity generated is quite low. The aim will be to avoid losing heat and to increase as much as possible the efficiency of the device. This would require increasing its performance by incorporating heat sinks. In addition insulation must be considered to ensure no carry-over of heat flow from the heat source to the cold sink.

4.1. Design

Conceptually the thermoelectric device is designed to generate electricity. The goal is to collect as much as possible heat from the combustion chamber of the stove, pump through the heat converter (TEG) and release the collected heat into the ambient air.

The requirements for the thermoelectric device are to be small, robust, inexpensive, light and portable as possible. The entire generator prototype is shown in Figure 29. The details of the general design are provided in Appendix D.

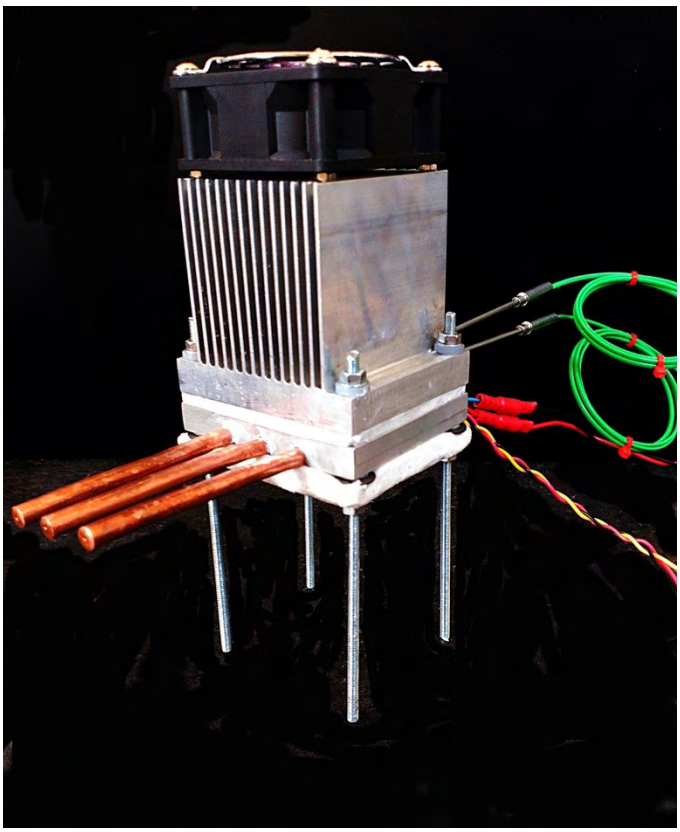

Figure 29: Thermoelectric generator prototype

4.2. Construction

To build the thermoelectric device a part list has been compiled and technical drawings of the device have been sent to the workshop in the mechanical engineering department of Trinity College for manufacture.

TEG module

The first part of the construction involved selecting a thermoelectric module. The TEG12-8 manufactured by *Marlow industries* was chosen for the application. The reason for choosing this TEG was that:

- It suited in the operating temperature range
- Its generated high output power and voltage was sufficient to power the fan
- It is small in size and thus heat transfer through the module is reduced
- All its electrical characterisation had been already studied in the previous section

Heat source

The prototype is supposed to collect heat from the combustion chamber of a cook stove. Due to the safety laboratory regulations and the difficulty of measuring the accurate power dissipated during the combustion, a quartz infrared heating element was used instead. This element is employed to provide the combustion scenario where most heat is transferred by radiation and convection.

The quartz infrared heating element is manufactured by *Ceramicx* (HQE500 model). It provides medium wave infrared radiation and allows a rapid heater response. The dimensions are 124x62.5x22 mm and it supplies 500 W of power.

Heat sink

In TEM power generation, no system is complete without a means of heat sinking or dissipating of the waste heat from the cold side. As shown in Figure 29 the heat was dissipated into the ambient environment via heat sink with aluminium fins. The heat sink was obtained from an old computer DELL 9y692; the size and shape were modified to fit in the device. As the base temperature rises at the cold sink, additional output power is released and the heat sink requires more heat to be released into the environment. Consequently, to minimize the temperature rise in the heat sink a 5V blower fan was used (Model KD0505PHS2 by *Sunon*). The fan would be powered by the thermoelectric generator.

Heat pipes

The prototype must be placed apart from the heat source; consequently an effective heat conductor was needed. The aim of the heat pipes is to collect heat from the infrared heating element and to transfer it to the hot plate. Heat pipes are used due to its high thermal conduction. They can exhibit a performance which exceeds that of an equivalent sized component made from pure copper by over 1000 times (27).

Several considerations were taken into account to select the type of heat pipes:

- Heat transport limitation
- Working fluid appropriate for the application
- Wick structure
- Length and diameter

Finally, the model 00C93470101 manufactured by *CCI* was chosen. The main properties are shown in table 3.

Working fluid	Water
Pipe material	Copper
Wick structure	Sintered-grooved composite
Length	150 mm
Diameter	6mm
Power Rating	80 W

Table 3: Main properties of heat pipes

Mounting Heat pipes in the hot aluminium plate

Heat pipes can be mounted to the hot base in several ways, including direct soldering into grooves or adhesively bonded into the metallic base. Because of an aluminium plate is used soldering was not a good option.

Finally, the decision was to extrude with groves the aluminium plate for allowing heat pipes to be mechanically clamped into the groves. To have an extra-efficient metal to metal thermal interface the heat pipes were put under pressure into the aluminium plate as shown in Figure 30.

Figure 30: Heat pipes mounted in hot aluminium plate